Pendred Syndrome in Two Galician Families: Insights into Clinical Phenotypes through Cellular, Genetic, and Molecular Studies

Fernando Palos,* María E. R. García-Rendueles, David Araujo-Vilar, Maria Jesús Obregon, Rosa Maria Calvo, Jose Cameselle-Teijeiro, Susana B. Bravo, Oscar Perez-Guerra, Lourdes Loidi, Barbara Czarnocka, Paula Alvarez, Samuel Refetoff, Lourdes Dominguez-Gerpe, Clara V. Alvarez, and Joaquin Lado-Abeal

Unidade de Enfermedades Tiroideas e Metabólicas (F.P., D.A.-V., O.P.-G., L.D.-G., J.L.-A.), Department of Medicine, and Departments of Physiology (M.E.R.G.-R., S.B.B., C.V.A.) and Pathology (J.C.-T.), Fundación Pública Gallega de Medicina Genómica (L.L.), Molecular Medicine Unit, Complejo Hospitalario Universitario de Santiago, Servicio Galego de Saude, University of Santiago de Compostela, Santiago de Compostela 15075, Spain; Instituto de Investigaciones Biomédicas "Alberto Sols" (M.J.O., R.M.C.), Consejo Superior de Investigaciones Científicas and Universidad Autónoma de Madrid, 28049 Madrid, Spain; Fundación Pública Hospital Virxen da Xunqueira (P.A., J.L.-A.), Servicio Gallego de Salud, 15270 Cee, Spain; Department of Biochemistry (B.C.), Medical Centre for Postgraduate Education, 02-813 Warsaw, Poland; and Department of Medicine and Pediatrics (S.R.), Committees on Genetics and Molecular Medicine and J. P. Kennedy Mental Retardation and Developmental Disabilities Center, The University of Chicago, Chicago, Illinois 60637

Context: We studied two families from Galicia (northwest Spain) with Pendred syndrome (PS) and unusual thyroid phenotypes. In family A, the proposita had a large goiter and hypothyroxinemia but normal TSH and free T_3 (FT_3). In family B, some affected members showed deafness but not goiter.

Objective: Our objective was to identify the mutations causing PS and molecular mechanisms underlying the thyroid phenotypes.

Interventions: Interventions included extraction of DNA and of thyroid tissue.

Patients: Propositi and 10 members of the two families participated in the study.

Main Outcome Measures: Main outcome measures included *SLC26A4* gene analysis, deiodinase activities in thyroid tissue, and c.416–1G→A effects on *SLC26A4* splicing. In addition, a primary PS thyrocyte culture, T-PS2, was obtained from propositus B and compared with another culture of normal human thyrocytes, NT, by Western blotting, confocal microscopy, and iodine uptake kinetics.

Results: Proposita A was heterozygous for c.578C→T and c.279delT, presented with goiter, and had normal TSH and FT_3 but low FT_4 attributable to high type 1 and type 2 iodothyronine deiodinase activities in the goiter. Propositus B bore c.279delT and a novel mutation c.416–1G→A; some deaf relatives were homozygous for c.416–1G→A but did not present goiter. The c.279delT mutation was associated with identical haplotype in the two families. T-PS2 showed truncated pendrin retained intracellularly and high iodine uptake with low efflux leading to iodine retention.

Conclusions: c.279delT is a founder mutation in Galicia. Proposita A adapted to poor organification by increasing deiodinase activities in the goiter, avoiding hypothyroidism. Lack of goiter in subjects homozygous for c.416–1G→A was due to incomplete penetrance allowing synthesis of some wild-type pendrin. Intracellular iodine retention, as seen in T-PS2, could play a role in thyroid alterations in PS. (***J Clin Endocrinol Metab* 93: 267–277, 2008**)

Pendred syndrome (PS) is an autosomal recessive disorder characterized by congenital sensorineural hearing loss and goiter without or with hypothyroidism (1). *SLC26A4* (solute carrier family 26, member 4), the PS gene (2), encodes a transmembrane protein (pendrin) expressed in the thyroid gland, inner ear, endometrium, and kidney, where it is involved in iodide,

0021-972X/08/$15.00/0

Printed in U.S.A.

doi: 10.1210/jc.2007-0539 Received March 9, 2007. Accepted October 9, 2007.

First Published Online October 16, 2007

* F.P. and M.E.R.G.-R. contributed equally to this study.

Abbreviations: CK, Cytokeratin; D1, type 1 deiodinase; DAPI, 4′,6-diamidino-2-phenylindole; ER, endoplasmic reticulum; FT_4, free T_4; NIS, sodium-iodide symporter; PS, Pendred syndrome; Tg, thyroglobulin; TPO, thyroperoxidase.

chloride, formate, and nitrate transport (3). *SLC26A4* mutations are also implicated in neurosensory nonsyndromic recessive deafness 4, DFNB4, with inner ear malformations (4, 5). Around 150 mutations in *SLC26A4* have been reported (http://www.medicine.uiowa.edu/pendredandbor/listed_mutations.htm). Different populations are affected by different mutations, and founder mutations have been reported in a few cases (4–17).

In the thyroid gland, pendrin acts at the apical pole of thyrocytes to transport intracellular iodide into the follicular lumen (18). Loss of pendrin function causes a failure in iodine supply and an organification defect often leading to euthyroid goiters (8, 10, 12, 16, 19) similar to those seen in iodine-deficient areas (20). We report two unrelated families with PS who have a thymidine deletion c.279delT at exon 3, resulting from a founder mutation. A thyrocyte cell line, T-PS2, was obtained from a primary thyroid culture of the family B propositus, providing data on the effects of the c.279delT and c.416–1G→A mutations on mutated pendrin localization and iodine handling in affected thyrocytes.

Subjects and Methods

Subjects

Family A

The proposita was a 43-yr-old deaf woman with grade III asymmetric multinodular goiter (Fig. 1). Neither her parents nor her three siblings were deaf. Although serum free T_4 (FT_4) was low (0.51 ng/dl, 6.56 pmol/liter; normal range 0.85–1.69 ng/dl), her serum TSH, FT_3, and rT_3 were normal; serum thyroglobulin (Tg) was 1312 ng/ml (normal range 0–80 ng/ml), anti-thyroperoxidase (anti-TPO) and anti-Tg antibodies were negative, and urine iodine was 102 μg/liter (median value for her age in our population is 79.7 μg/liter). A computer tomography scan showed enlarged vestibular aqueducts. A perchlorate test showed an organification defect. Increasing daily doses of L-thyroxine (25, 50, 75, and 100 μg) were given, but her serum FT_4 levels remained low or low-normal. A total thyroidectomy was performed (Fig. 1), and the patient was discharged on 100 μg L-thyroxine daily.

Family B

The propositus, a 26-yr-old deaf male, was referred to us for hypothyroidism. He was the only child of a nonconsanguineous deaf couple

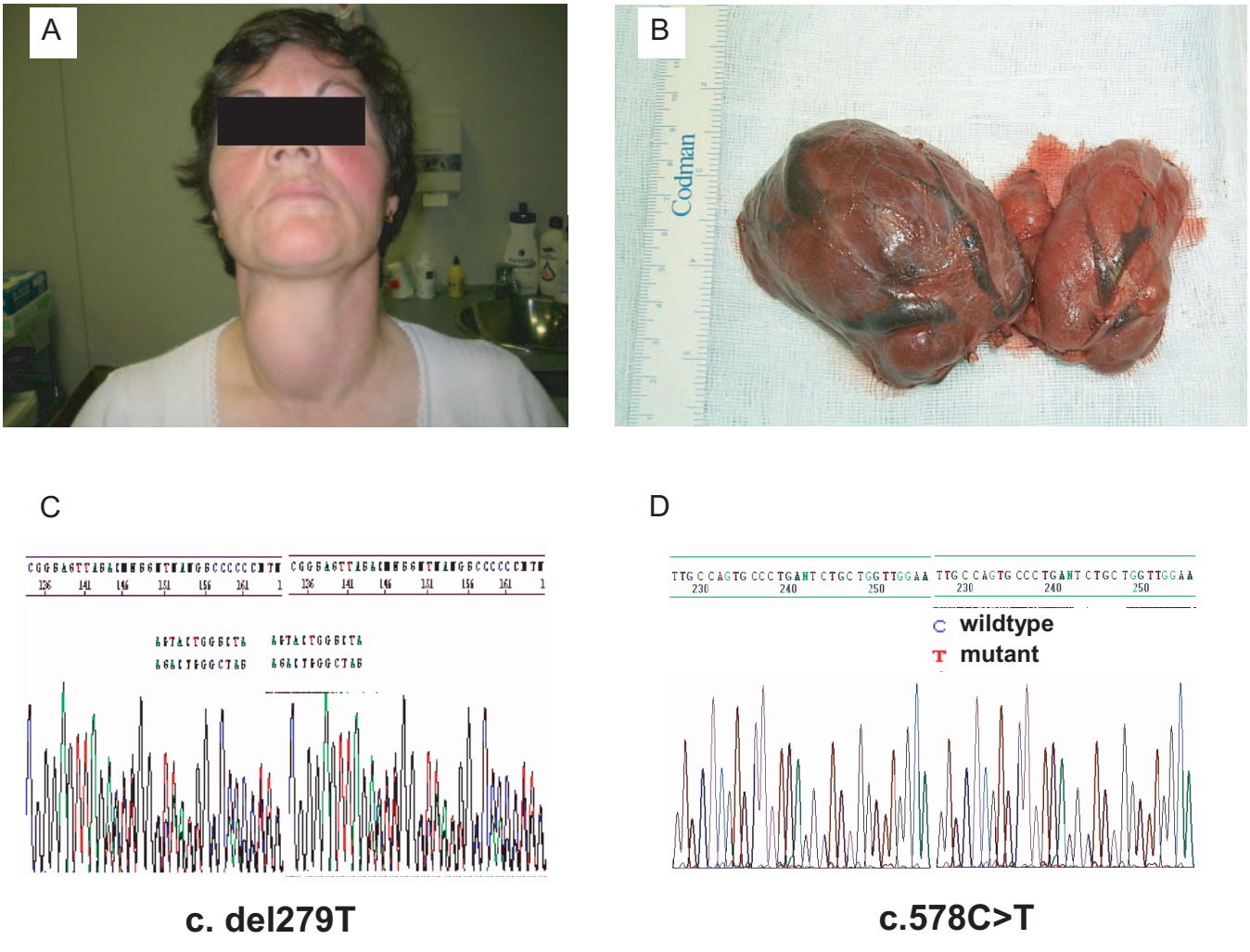

FIG. 1. A, The proposita of family A, a 43-yr-old woman with deafness and a large goiter; B, gross appearance of thyroid at surgery showing multinodular goiter with larger nodules in the right lobe; C and D, the proposita was compound heterozygous for c.279delT, a frameshift mutation at exon 3 (C), and c.578C→T at exon 5 (D).

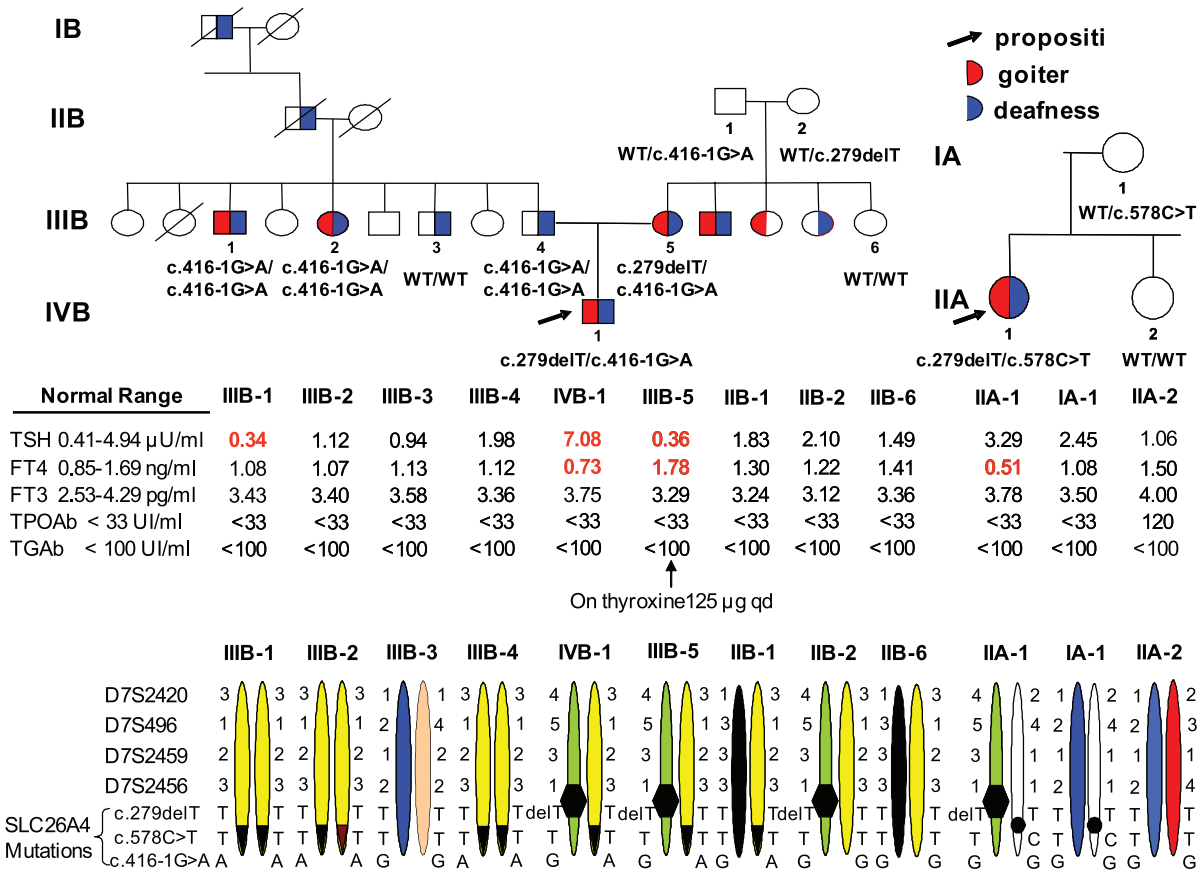

FIG. 2. *Top*, Family pedigrees. Phenotypes are indicated within each *symbol*, and genotypes and results of thyroid function tests appear *below* each of the family members studied. Abnormal values are in *bold numbers*. *Roman numbers* indicate family generation, and *Arabic numbers* indicate studied family members. *Bottom*, Haplotypes. Carriers of c.279delT share a common haplotype not observed in noncarrier members, suggesting a founder effect. In family B, the novel mutation c.416–1G→A was found in the propositus' maternal grandfather, mother, father, and two paternal siblings. c.416–1G→A carrier and noncarrier members of family B share a common haplotype not present in family A.

with a strong family history of deafness and goiter (Fig. 2). He had a goiter with a 1-cm nodule in the right lobe. Serum TSH was 7.08 μU/ml, with low FT_4 (0.73 ng/dl, 9.40 pmol/liter) and normal FT_3. Anti-TPO and -Tg antibodies were negative. A fine-needle aspiration cytology was suggestive of follicular neoplasia, and a right hemithyroidectomy was performed. The propositus' mother had a grade II goiter, whereas his father had neither goiter nor abnormal serum levels of thyroid hormone, although a perchlorate test did show a partial organification defect. Both parents presented with profound neonatal deafness, as did two of the mother's four siblings and two of the father's seven siblings. One of the father's brothers (subject IIIB.3, Fig. 2) showed much less severe deafness starting in childhood.

Genetic studies

Genomic DNA was extracted from blood cells of the propositi, 10 members of their families, and 50 normal volunteers (age range 20–60 yr) and from thyroid tissues of the propositi and 60 control subjects (healthy parts of surgically removed multinodular goiters). All exons of the *SLC26A4* gene were amplified by PCR (primer sequences and PCR conditions available upon request) and sequenced in an ABI PRISM 3100 (Applied Biosystems, Foster City, CA). The study was approved by our Institutional Review Board, and informed consents were obtained.

For haplotype analysis, four polymorphic markers closely linked to *SLC26A4* were genotyped. According to the NCBI STS map, *D7S2459* is located in *SLC26A4* intron 10, and *D7S2420* and *D7S496* are proximal and *D7S2456* distal to *SLC26A4*. Oligonucleotide primer sequences were obtained from http://www.ncbi.nlm.nih.gov, and forward primers were fluorescence labeled. PCR products were electrophoresed in a MegaBace 500 (Amersham Pharmacia Biotech, Piscataway, NJ). Alleles were numbered according to product size.

Effects of the intronic mutation on *SLC26A4* were investigated in skin fibroblasts and thyroid tissue from the B propositus. cDNA fragments spanning from exon 3 to exon 6 were PCR amplified and cloned into a pGEMT-Easy vector (Promega, Madison, WI), and the products were sequenced as described.

Determination of type 1 and type 2 iodothyronine deiodinases (D1 and D2) and MCT8

D1, D2, and MCT8 mRNA levels and D1 and D2 activities were measured in thyroid tissue from the A proposita and from healthy parts of six surgically derived thyroid specimens and two toxic follicular adenomas.

MCT8, D1, and D2 mRNAs and the internal control RNA polymerase II were quantified in a Light Cycler 2.0 (Roche, Indianapolis, IN) using specific probes and oligonucleotide primers designed by Universal ProbeLibrary (Roche). Real-time PCR conditions are available upon request. Results were normalized for RNA polymerase II, using the $2^{-\Delta\Delta CT}$ method (21).

D1 and D2 activities were measured in thyroid tissue homogenates as described (22, 23).

Thyroid hormone levels in thyroid gland samples were determined by in-house RIAs (24).

TABLE 1. mRNA transcript analysis of cDNA from the family-B propositus

Allele	mRNA transcript		Expected protein
	Size (bp)	Mutation	
r.279delT			
1	499	r279delt	Premature stop
r.416−1g→a			
2	500	Normal splice (no mutation)	Wild-type pendrin
3	499	Abnormal splice, 416_417del	Premature stop
4	420	Abnormal splice, 416_495del	Premature stop
5	417	Abnormal splice, 416_498del	Premature stop

Histological and immunohistochemical studies

Immunohistochemical studies were performed on paraffin sections of thyroid specimens from the two propositi using an EnVision peroxidase/diaminobenzidine kit with antibodies to thyroid transcription factor-1 (Dako, Carpinteria, CA; dilution 1:50), Tg (Tg6, 1:2000; Dako), TPO (MoAb47, 1:50; Dako), calcitonin (polyclonal, 1:1000; BioGenex, San Ramon, CA), cytokeratin (CK) 7 (OV-TL 12/30, 1:50; Dako), CK1–CK8, CK10, CK13, CK14, CK16, and CK19 (AE1–AE3, 1:20; Dako), CK20 (Ks 20.8, 1:20; Dako), vimentin (V9, 1:5000; BioGenex), and galectin-3 (9C4, 1:200; Novocastra, Newcastle upon Tyne, UK). An affinity-purified antibody against pendrin, PS1Ab (1:20), recognizing the first 15 amino acids of human pendrin, denominated pendrin1 (25), was also used. Negative controls in which the primary antibodies were replaced by nonimmune mouse serum, and positive controls such as normal thyroid tissue from autopsy and surgical thyroid tissue from a subject with Graves' disease, were included.

Cell culture, immunoblotting, and immunofluorescence analysis

Thyrocyte cell lines from the B propositus thyroid gland (T-PS2), from a normal thyroid tissue specimen (NT), and from a cold follicular adenoma (T-FA6) were obtained as previously described (26).

Amounts of the sodium-iodide symporter (NIS) and pendrin were estimated by Western blot of protein extracts. Low-detergent extracts to assess cytoplasmic membrane contents [endoplasmic reticulum (ER) and Golgi], and total extracts to include plasma membrane proteins, were prepared as described (27, 28). Immunodetection was carried out with antibodies to NIS (1:300; Chemicon, Temecula, CA), PS1Ab (1:300) and tubulin (1:5000; Sigma Chemical Co., St. Louis, MO). Bound antibodies were detected with alkaline phosphatase-labeled secondary antibodies (Tropix, Bedford, MA).

Immunofluorescence assays were done in cells seeded onto glass coverslips, fixed with 1% paraformaldehyde for 20 min, permeabilized with Triton 1% for 10 min at room temperature, and then quenched with 50 mM NH_4Cl for 1 h. Alternatively, cells were fixed with ice-cold methanol for 10 min. Antibodies used were the Chemicon anti-NIS (1:50) and PS1Ab (1:20, methanol-fixed cells) or PS5Ab, which recognizes the last 13 carboxyl-terminal amino acids of human pendrin, denominated pendrin5 (1:20, paraformaldehyde-fixed cells) (25). Thyrocytes were identified by Tg immunofluorescence (Novocastra; 1:65). The nucleus was counterstained with 4′,6-diamidino-2-phenylindole (DAPI) (Sigma; 1:100).

Iodide uptake

Iodide uptake was measured according to Dohan *et al.* (29) with minor modifications, using T-PS2 and NT cells grown in 24-well plates. For steady-state experiments, incubations proceeded for 30 min with 20 or 40 μM $Na^{125}I$. For time-course analysis, cells were incubated for 30 sec and 1, 2, 5, 10, 15, and 30 min. For dose-response experiments, cells were incubated for 30 sec and 5, 30, and 60 min with 0.1, 0.25, 0.5, 1.25, 2.5, 5, 10, 20, or 40 μM NaI. Cells were lysed by adding 200 μl 1 M NaOH to each well for 10 min at room temperature. ^{125}I in cells was then quantitated in a γ-scintillation counter. Cells from replicate wells were counted to express I^- uptake as picomoles per 10^5 cells. $NaClO_4$ (40 μM) was added to inhibit I^- uptake when appropriate.

For efflux experiments, cells were loaded with 20 μM $Na^{125}I$ for 30 min and washed (29); some replicates were terminated at this point (intracellular ^{125}I content 100%), whereas in the other replicates, the medium was replaced at 5, 15, and 25 min as described (29). Radioactive medium was quantitated, and results are expressed as percentage of intracellular content. Finally, cells were lysed for quantitation of ^{125}I.

Kinetic curves were fitted by nonlinear least-square regression using GraphPad Prism software based on the Michaelis-Menten equation. All parameters were determined at least in triplicate in three independent experiments.

TABLE 2. Relative mRNA expression of deiodinases and MCT8, and deiodinase activities, in the family-A proposita and control thyroid tissues.

Sample	Relative mRNA expression			Enzymatic activity	
	MCT8	D1	D2	D1 (pmol/min·mg protein)	D2 (fmol/h·mg protein)
Family A proposita	1.00 ± 0.05	1.00 ± 0.07	1.00 ± 0.08	70.7 ± 0.1	166.5 ± 34.9
1	0.93 ± 0.09	0.37 ± 0.05[a]	0.54 ± 0.10[a]	11.2 ± 1.6[a]	86.3 ± 18.8[a]
2	0.36 ± 0.03[a]	0.11 ± 0.01[a]	0.16 ± 0.12[a]	ND	ND
3	0.45 ± 0.02[a]	0.24 ± 0.01[a]	0.21 ± 0.03[a]	6.8 ± 0.3[a]	32.5 ± 5.3[a]
3T	0.99 ± 0.20	0.64 ± 0.11	0.29 ± 0.06[a]	45.4 ± 3.8[a]	132.9 ± 12
4T	1.09 ± 0.36	1.10 ± 0.20	0.37 ± 0.01[a]	142 ± 4.3[b]	180 ± 2
5	0.30 ± 0.03[a]	0.26 ± 0.02[a]	0.55 ± 0.10[a]	24.7 ± 4.3[a]	54.8 ± 22.7[a]
6	1.63 ± 0.04[b]	0.78 ± 0.07	0.59 ± 0.17	34.2 ± 4.1[a]	150.7 ± 0.6
7	0.91 ± 0.01	0.55 ± 0.22	0.18 ± 0.14[a]	ND	ND

Data are shown as means ± SD. Numbers 1–7 refer to healthy parts of surgically derived thyroid specimens. ND, Not done; T, thyroid tissue from inside a toxic adenoma.

[a] $P < 0.05$ *vs.* family-A proposita.

[b] $P < 0.05$ *vs.* family-A proposita with higher values than the family-A proposita.

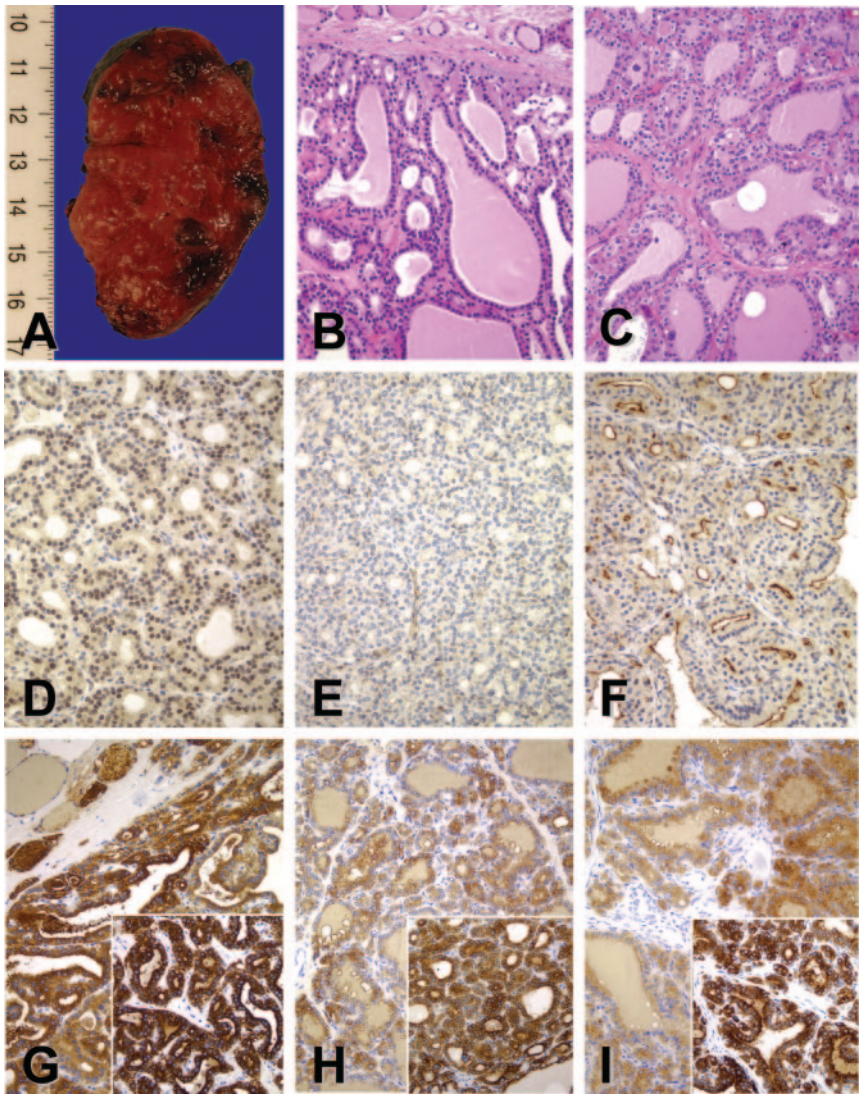

FIG. 3. A, Gross appearance of right thyroid lobe from the propositus of family B; B and C, hematoxylin-eosin stain of thyroid tissue from the propositi of family A (B) and family B (C); D and E, lack of apical membrane staining for pendrin with PS1Ab, an antibody against the first 15 amino acids of human pendrin, with perinuclear enhanced halo in thyroid follicle cells from the propositi of family A (D) and weak cytoplasmic staining in family B (E); F, strong apical membrane PS1Ab staining is seen in Graves' disease; G–I, Tg and TPO immunoreactivity (*inset*) was found in both propositi and control thyroid glands: the proposita of family A (G), the propositus of family B (H), and Graves' disease (I). All original magnifications, ×200.

Thyroid function tests

TSH, FT_4, and FT_3 were measured by chemiluminescence using ADVIA Centaur (Bayer Diagnostics, Tarrytown, NY). Tg, TgAb, and TPOAb were measured using Immulite 2000 (Diagnostic Products Corp., Los Angeles, CA). rT_3 was measured by RIA (Biocode Hycel, Liege, Belgium).

Statistical analysis

One-way ANOVA with *post hoc* comparisons by Student's *t* test and the Wilcoxon signed-rank test were used for statistical analysis.

Results

Genetic studies

The family-A proposita was heterozygous for c.279delT and c.578C→T. Mutation c.279delT, a thymidine deletion located in exon 3 (Fig. 1C), causes a frameshift that introduces a stop codon three amino acids downstream (p.Ser93ArgfsX3). Mutation c.578C→T (Fig. 1D), located in exon 5, results in replacement of the normal threonine with an isoleucine at codon 193 (p.Thr193Ile) in the third membrane region of pendrin. The proposita inherited mutation c.578C→T from her mother. No mutations were found in the proposita's sister, and no DNA samples were available from her father or two brothers.

The family B propositus was heterozygous for c.279delT (see above) and for c.416–1G→A, located at the acceptor splice site of intron 4, leading to replacement of the normal guanosine with an adenosine. His mother had the same compound heterozygous genotype (c.279delT, c.416–1G→A) and his father was homozygous for c.416–1G→A (Fig. 2). Two of the father's siblings (IIIB.1 and IIIB.2, Fig. 2) showed profound deafness and were homozygous for c.416–1G→A. Subject IIIB.3 (Fig. 2) did not have SLC26A4 mutations and showed much less severe deafness.

Mutations c.279delT, c.578C→T, and c.416–1G→A were not found in 120 alleles from 60 normal thyroid tissue samples obtained from Galician patients or in 100 alleles from 50 blood samples obtained from normal Galician volunteers aged between 20 and 60 yr.

Members of the two families bearing c.279delT shared the same haplotype, which was not present in unaffected individuals (Fig. 2). Regarding c.416–1G→A, both affected and unaffected members of family B share a common haplotype not found in family A (Fig. 2).

PCR amplification of propositus B thyroid *SLC26A4* cDNA, extending from exon 3 to exon 6, gave the expected 500-bp product and a 420-bp product. A similar result was obtained using fibroblast cDNA from this propositus. In control thyroid tissue, only a 500-bp product was observed. The 500-bp fragment corresponded to three transcripts (Table 1): a 499-bp transcript [r.279delt (37.5%)] resulting from thymidine deletion at nucleotide 279, a 499-bp transcript [r.416–1 g→a;416_417del (25%)] resulting from an abnormal splicing one base from the regular splicing site, and an unexpected 500-bp wild-type transcript (37.5%). The 420-bp fragment likewise corresponded to two transcripts, of 420 and 417 bp, that resulted from abnormal splicing 79 and 82 bp from the regular site (r.416–1 g→a; 416_495del, 416_498del). All the abnormal transcripts introduced premature stop codons.

Deiodinase and MCT8 levels

Deiodinase mRNA expression and activities were higher in the thyroid gland of the A proposita than in most control thyroid tissues (Table 2). MCT8 mRNA expression was also high in the proposita's thyroid (Table 2). Thyroid hormone contents in con-

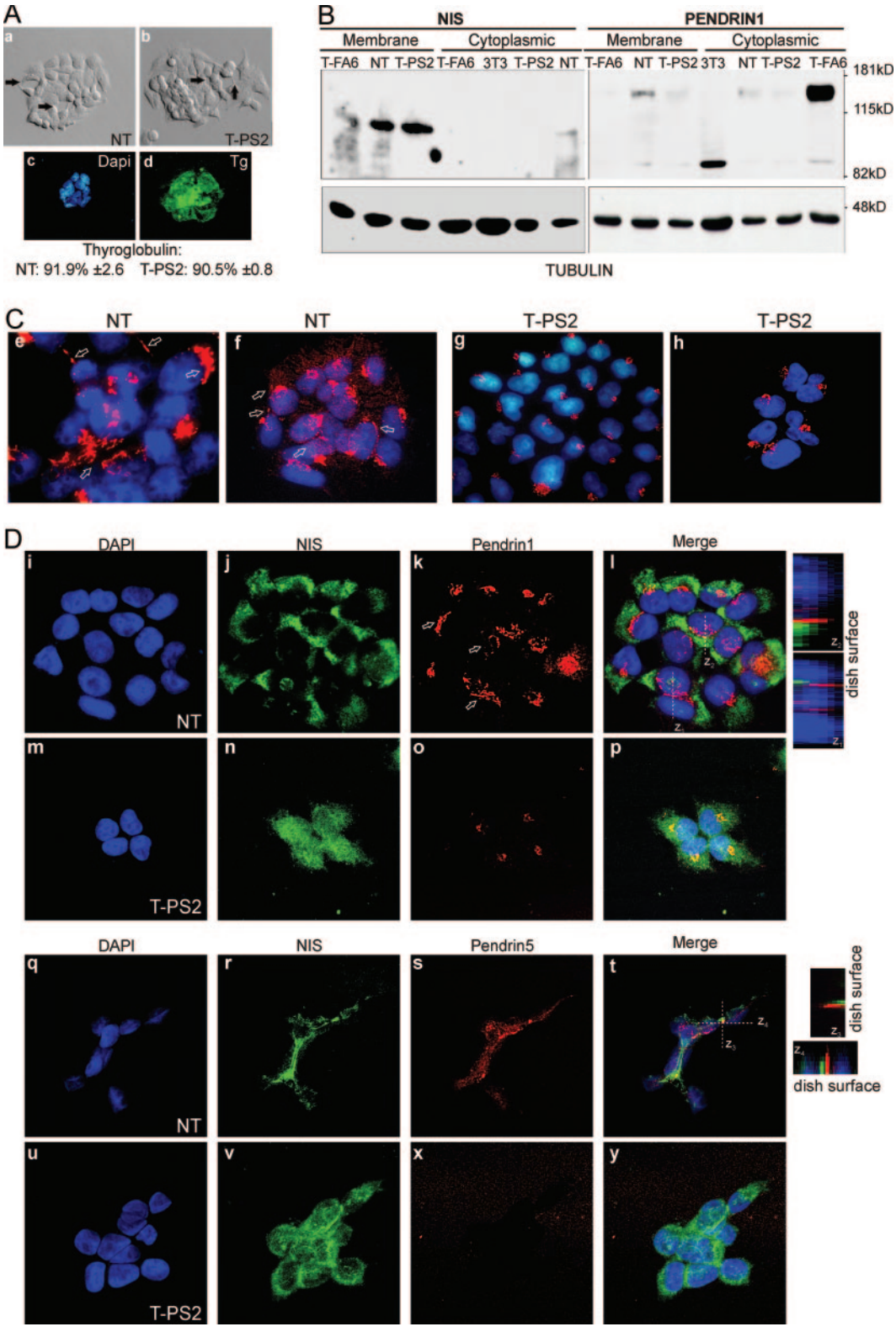

FIG. 4. At the outer plasma membrane, normal thyrocytes (NT) express fully glycosylated NIS and pendrin, whereas cells from the propositus of family B (T-PS2) express only NIS. A, The appearance of cultured NT (a) and T-PS2 cells (b) is similar under the phase-contrast microscope. The cells are small and polygonal and leave round spaces between them, recalling a follicular structure (see *arrows*). In both cell lines, using DAPI for nuclear counterstaining, practically all cells expressed Tg (shown for T-PS2, c and d). B, Western blotting against NIS (*left*) and pendrin (*right*) using hot SDS extracts enriched in plasma membrane proteins (membrane) or 1% Triton extracts with intracellular membrane content, *i.e.* Golgi or ER (cytoplasmic). As a loading control, the membranes were rehybridized against tubulin. NIS is expressed mainly as the 100-kDa fully glycosylated form at the plasma membrane in NT, T-PS2, and the T-FA6 primary-culture follicular adenoma line from our BANTTIC collection; smaller bands around 80 kDa correspond to nonglycosylated immature NIS. Intracellular levels are undetectable in all lines except NT, in which a faint band can be seen suggesting slightly greater NIS expression. Mouse 3T3 fibroblasts were used as negative control. NT cells express the 130-kDa fully glycosylated pendrin at the plasma membrane, but only a very weak band (less than 5%) can be seen in T-PS2 and T-FA6 cells. The faint 85-kDa band is the nonglycosylated protein. In

trol thyroid glands were 2–160 μg/g for T_4 and 2–42 μg/g for T_3. In the proposita's thyroid, T_4 and T_3 content was 0.09 and 0.05 μg/g, respectively.

Histology and immunohistochemistry

Thyroid glands from the two propositi showed similar microscopic appearance (Fig. 3). The thyroid tissue and hyperplastic nodules were hypercellular, with normal and microfollicular areas along with some fibrous septae. Tall columnar cells in the follicles and scattered cells with nuclear atypia, characterized by enlargement and hyperchromasia, were also seen. Immunohistochemical findings were likewise similar in the two propositi (Fig. 3); follicular cells contained thyroid transcription factor-1, Tg, TPO, CK (CK7, AE1–AE3), and vimentin and were negative for calcitonin, CK20, and galectin-3.

Follicles from normal thyroid gland and from Graves' disease (Fig. 3F) showed pendrin1 immunoreactivity (PS1Ab) in the luminal/apical border. Thyroid tissue from proposita B was negative at the apical membrane and weakly stained follicular cytoplasm (Fig. 3E), suggesting that truncated proteins from alleles c.279delT and c.416–1G→A were either unstable or down-regulated. Thyroid tissue from proposita A was negative at the apical membrane but presented a perinuclear enhanced halo (Fig. 3D), suggesting that full-length pendrin from allele c.578C→T was stable although retained in intracellular perinuclear organelles (ER and Golgi).

Cell cultures, immunoblotting, and immunofluorescence analysis

T-PS2, a thyrocyte cell line compound heterozygous for c.279delT and c.416–1G→A, was obtained from a thyroid specimen of the B propositus and compared with a line of normal human thyrocytes, NT, from our bank (BANTTIC) (26, 27). Both cell lines have similar polygonal epithelial appearance, making follicle-like rounded structures (see Fig. 4A, a and b). More than 90% of the thyrocytes in both lines expressed Tg (Fig. 4A, c and d). Doubling times were also similar (around 23 h).

The NT and T-PS2 cell lines showed similar levels of glycosylated plasma-membrane NIS (Fig. 4B), higher than T-FA6 cells (Fig. 4B). NT cells showed high levels of glycosylated plasma-membrane pendrin (around 130 kDa) and a weaker cytoplasmic band corresponding to pendrin in the process of sorting (Fig. 4B). A smaller band around 85 kDa corresponds to nonglycosylated immature pendrin. T-PS2 cells showed a very weak band of glycosylated pendrin, in both membrane and cytoplasmic extracts, suggesting intracellular retention of the scarce normal pendrin (Fig. 4B). Negative control 3T3 mouse fibroblasts did not express pendrin, but a smaller band around 80 kDa was observed (Fig. 4B). Interestingly, T-FA6 cells that expressed a faint band at the plasma membrane showed strong intracellular expression of pendrin (Fig. 4B). The presence of a small quantity of normal protein agrees with the results mentioned above on the effect of c.416–1G→A on *SLC26A4* splicing (see Table 1); as noted, mutation c.416–1G→A showed incomplete penetrance leading to a marked decrease but not complete disappearance of the normal pendrin transcript.

Confocal immunofluorescence studies with PS1Ab showed staining of NT thyrocytes at a point near the nucleus in the Golgi location and in narrow lines typical of plasma membrane localization (Fig. 4C, e and f). Almost all T-PS2 thyrocytes showed the spot near the nucleus (Fig. 4C, g and h), but no lines were detected, indicating either that normal and truncated proteins were both retained in the Golgi or that the concentration of normal pendrin is very low at the membrane. Recent results in our laboratory have shown low levels of pendrin mRNA expression in T-PS2 compared with NT (unpublished results), suggesting that the weak membrane expression of pendrin in T-PS2 could be related not only to defective membrane targeting but also to low transcription levels of the pendrin mutants.

We also studied the colocalization of NIS and pendrin (using PS1Ab against pendrin1 and PS5Ab against pendrin5). In normal thyrocytes, both NIS and pendrin1 showed a linear staining typical of plasma membrane localization (Fig. 4D, i–l). However, the two proteins were usually not expressed in the same membrane patches, as can be seen from the scarce colocalization in the projections and the z planes. In T-PS2 thyrocytes, NIS was also located in the plasma membrane, but pendrin1 showed very few spots outside the Golgi (Fig. 4D, m–p). Next, we repeated the colocalization studies using PS5Ab, recognizing the last 13 carboxyl-terminal amino acids of human pendrin. In these studies, both NIS and pendrin showed linear staining in the NT thyrocytes, but again, each protein localized in its plasma membrane region, with little colocalization (Fig. 4D, q–t). Although the cells were grown in monolayers, this arrangement recalls that of partially polarized thyrocytes. In the T-PS2 thyrocytes, despite the correctly localized membrane NIS, only weak pendrin spots were seen (Fig. 4D, u–y).

Iodide uptake

NT cells showed fast iodide uptake, with cellular iodide content plateauing at 2 min and not changing over the remainder of the 30-min experiment (Fig. 5A). The kinetics curve suggests that the two iodine transporters (NIS and pendrin) were working in opposite directions. NIS initiates iodide uptake, and once intra-

intracellular membranes, NT cells express a weak band corresponding to pendrin in the process of sorting, and T-PS2 cells likewise show only a weak band. However, T-FA6 cells retain pendrin intracellularly. C, Confocal immunofluorescence images using the same pendrin antibody as in B, PS1Ab (specific for the N-terminal part of the protein). DAPI is used to show nuclei. Both a ×40 water-immersion objective with ×3 magnification (e and g) and a ×63 oil-immersion objective with a ×1.5 magnification (f and h) were used. PS1Ab staining is localized in the Golgi (*round spots* beside the nuclei) and the plasma membrane (*straight lines* indicated by *arrows*) in normal thyrocytes (NT); in T-PS2 thyrocytes, pendrin appears to be retained in the Golgi (truncated proteins). D, Double immunofluorescence with NIS and PS1Ab shows intracellular and plasma membrane staining (*arrows*) of both proteins in NT (i–l, ×1000). Note that membrane colocalization is not frequent: the z projections obtained through stacking of confocal images show that, although localized in the membrane, the two proteins rarely coincide in the same locations, as indicated by the scarce *yellow spots*. T-PS2 cells (m–p, ×1000) show intracellular and plasma membrane staining of NIS, but only one isolated spot of pendrin can be seen at the plasma membrane, whereas the rest is retained in the Golgi. Similar double-immunofluorescence studies were performed using PS5Ab, specific for the C-terminal end of the pendrin protein. Both NIS and pendrin are localized at the plasma membrane in NT cells (q–t, ×1000), although both proteins seem to occupy different membrane domains (see z projections). In T-PS2 cells, the PS5Ab image is overexposed to demonstrate the absence of specific staining (u–y).

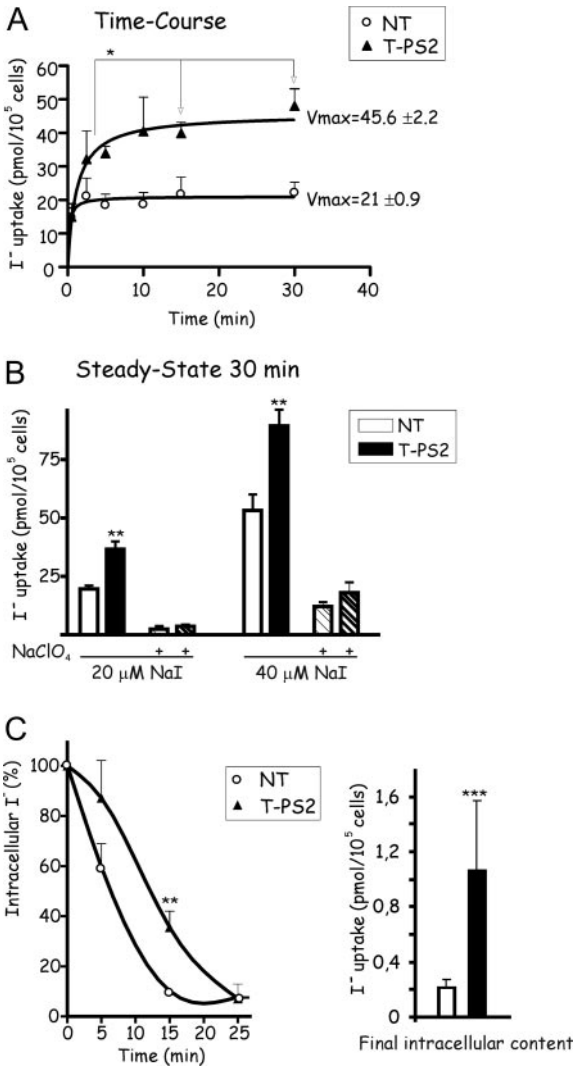

FIG. 5. T-PS2 thyrocytes take up iodide and retain it intracellularly. A, Time course of iodide uptake (20 μM NaI) by thyrocyte lines. Normal NT cells show fast uptake in the first 30 sec, reaching a plateau at 2 min, with no further changes in intracellular iodine content over the remainder of the 30-min experiment (r^2 = 0.65); the kinetic curve suggests that, during the first 2 min, NIS transports iodide into NT thyrocytes but that iodide is then effluxed from the cells through pendrin, with the two transporters (NIS and pendrin) then working in opposite directions to maintain equilibrium. In contrast, T-PS2 cells show a progressive increase in iodide uptake, reaching a plateau much later (r^2 = 0.99), suggesting a model with a single transporter (NIS); in fact, there were significant differences in intracellular iodine content between the time points 2 or 5 min and the time points 15 or 30 min. Vmax was twice as high for T-PS2 thyrocytes as for NT. B, Steady-state uptake of NaI after incubation for 30 min. At any given concentration of NaI, the intracellular iodide uptake by T-PS2 thyrocytes (*black bars*) was twice as high as by NT (*white bars*). In both cell lines, coincubation with 40 μM $NaClO_4$ blocked the iodide uptake (*striped bars*). C, Efflux of iodide into the culture medium expressed as a percentage of the amount obtained at time 0 after the steady-state uptake using 20 μM NaI. NT thyrocytes released all radioactive iodine to the medium after 15 min of initial washing. T-PS2 released the radioactive iodine much more slowly, so that after 15 min, 40% still remained inside the cells ($P < 0.01$). Efflux stopped at 25 min, but the residual amount inside the cell at that time was significantly higher in T-PS2 cells (*black bars*) than in NT cells (*white bars*).

cellular iodide concentration reaches a certain level, pendrin will start efflux, maintaining the amount of iodide inside the thyrocyte at a constrained level. In contrast, T-PS2 cells showed a progressive increase in iodide level, which plateaued at around 15 min (Fig. 5A), in accordance with a single transporter (NIS) model. Vmax was two times higher in T-PS2 than NT cells, suggesting that iodide was accumulated in T-PS2 thyrocytes. In fact, the steady-state uptake after 30 min was higher in T-PS2 than NT thyrocytes (Fig. 5B).

Efflux was faster from NT than from T-PS2 cells (Fig. 5C, *left*). At 5 min, 40% of radioactivity had already effluxed from NT cells, but no significant efflux was seen from T-PS2; by 15 min, almost all radioactivity had effluxed from NT cells, but 40% remained in T-PS2. When residual iodide was measured at the end of the experiment, T-PS2 cells maintained higher intracellular iodide than NT cells (Fig. 5C, *right*).

Dose-response curves showed that after 5 min, T-PS2 cells had already reached equilibrium for iodide uptake with a Michaelis-Menten constant (K_m) similar to that expected for NIS at equilibrium (22 $\pm$ 4.8 μM) (Fig. 6). In contrast, NT cells achieved equilibrium and the expected K_m for iodide uptake at 1 h. Except at very short times of incubation (30 sec), when Vmax was higher for NT cells, the Vmax was twice as high in T-PS2 thyrocytes at any given time. These results suggest that normal thyrocytes behave as a complex system in which both transporters (NIS and pendrin) need to reach equilibrium slowly and that intracellular iodide concentrations are not high; however, PS-affected thyrocytes accumulate iodine through NIS, and iodine leaves the cell inefficiently through other nonspecific transporters.

Discussion

Two Galician families with PS were studied. *SLC26A4* gene sequences showed two previously described mutations, c.279delT (8, 17) and c.578C→T (11, 16) and a novel mutation c.416–1G→A. Both families had the c.279delT mutation, and a common haplotype was seen only in c.279delT carriers, suggesting a founder effect for this mutation. Galicians have low genetic diversity in comparison with other European populations, and founder effects are not uncommon (30).

The c.416–1G→A mutation was present in family B. Although the parents denied that they were related, they were born in the same village, and a common haplotype for c.416-G→A was found in both affected and unaffected family B members but not in haplotyped members of family A. Until recently, the Galician population was organized in small and relatively isolated groups, and it is likely that the parents of propositus B have a common ancestor. The fact that this mutation has not been previously reported also suggests that c.416–1G→A originated in Galicia.

We believe that the phenotype of the A proposita (large goiter, normal serum TSH and FT_3, and hypothyroxinemia) is an adaptive response to poor organification. In experimental animals, iodine-deficient diet increases thyroid weight and favors the synthesis and secretion of T_3 resulting in an increase in serum and tissue T_3/T_4 ratio (31, 32). These changes are partially due to a TSH-independent increase in T_3 generation (32), which can lead to low serum T_4, with normal or slightly elevated T_3 and normal TSH (31). In our patient, due to the marked increase in thyroid gland size, the raised D1 and D2 levels were sufficient to maintain

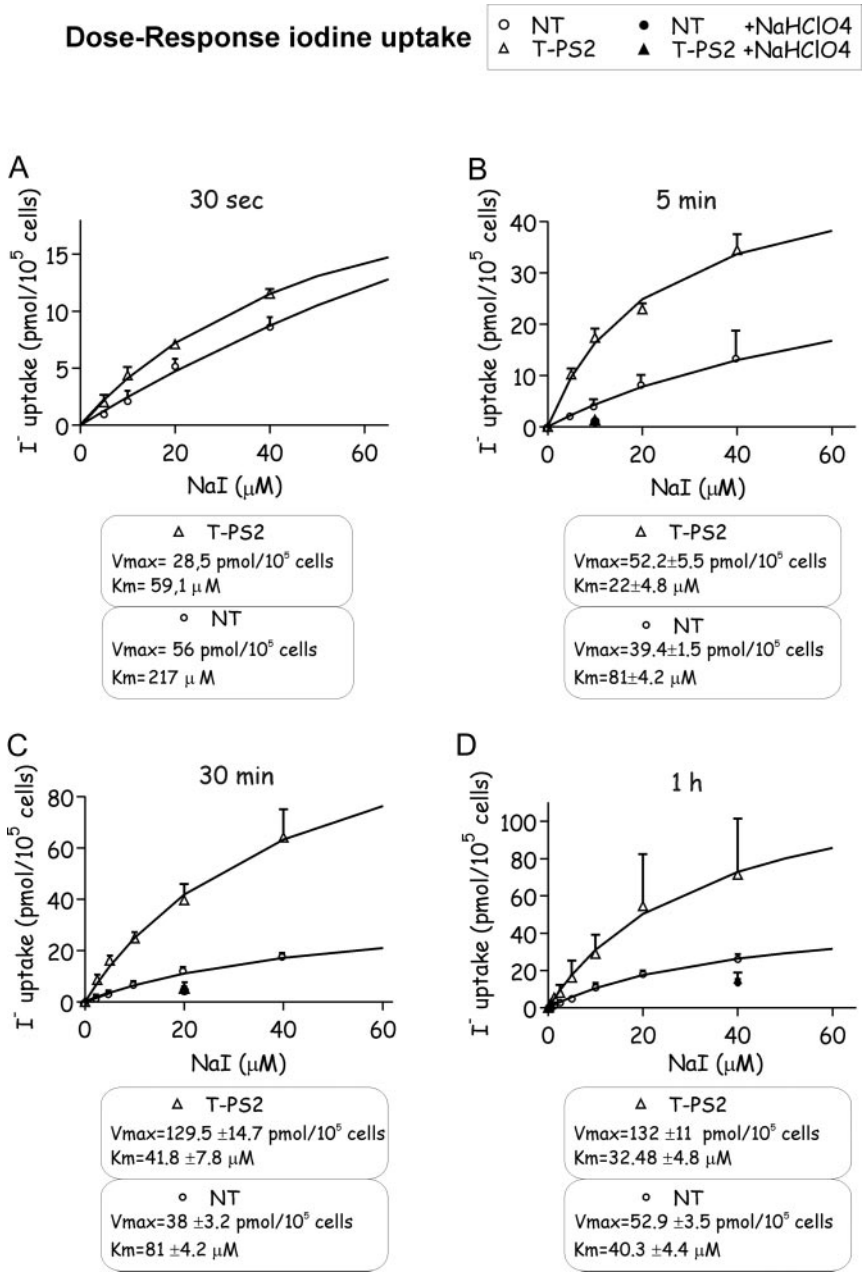

FIG. 6. Pendred thyrocytes quickly reach equilibrium for iodide uptake and progressively accumulate intracellular iodide. A–D, Intracellular iodide uptake by thyrocytes incubated with different NaI concentrations, at different times of incubation. Although at short incubation times (30 sec, A), the curves were similar for both lines, at 5 min (B), T-PS2 thyrocytes reached equilibrium with $K_m = 22 \pm 4.8$ μM, similar to the Michaelis-Menten constant at equilibrium for iodide uptake by NIS (K_m around 30–40 μM). In contrast, NT showed $K_m = 81 \pm 4.2$ μM, far above equilibrium. Similar behavior was maintained at 30 min (C), and at 1 h (D), NT thyrocytes finally reached equilibrium ($K_m = 40.3 \pm 4.4$ μM). Except at very short incubation times (30 sec), when Vmax was higher in NT cells, Vmax was about twice as high in T-PS2 thyrocytes at any given time. This result suggests that initially only the NIS transporter is working in NT, as in T-PS2, but that after a few seconds pendrin starts to work in NT, and equilibrium is reached later.

normal levels of serum FT_3. D1 and D2 will increase the intrathyroidal conversion of T_4 into T_3, and MCT8 will maintain the transport of thyroid hormones across thyrocytes. Interestingly, the proposita's L-thyroxine requirements were increased after thyroidectomy due to loss of the thyroid as a source of T_3. A transient increase in serum TSH in response to low thyroid hormone synthesis is a straightforward explanation for goiter development in PS patients, although other mechanisms could be involved. T-PS2 cells showed increased iodide retention leading to a steady intracellular iodide concentration. This finding suggests that intracellular accumulation of iodide may occur in thyrocytes of PS patients with adequate iodine intake, and this could have a role in the functional changes seen in diseased Pendred thyrocytes. High dietary iodine intake promotes goiter in humans (33), and although the mechanisms are not clearly defined, the Wolff-Chaikoff effect seems to play a role. However, a direct stimulating action of iodine on thyrocyte proliferation is also possible. Very high NaI concentrations (10–50 mM) over several days inhibited the proliferation of cultured rat FRTL-5 thyrocytes (34), but this was probably a toxic effect. In contrast, physiological concentrations (1 μM KI, equivalent to 150 μg/liter) stimulated basal and epidermal growth factor-induced proliferation in primary cultures of porcine follicles (35, 36) through down-regulation of intracellular cAMP levels.

Family B's clinical phenotype is complicated by the finding of deafness with and without *SLC26A4* mutations. Also, homozygotes for c.416–1G→A have congenital deafness, but not all have goiter. In fact, neither goiter nor thyroid hormone abnormalities were found in the father of the propositus, homozygous for c.416–1G→A. A similar situation has been recently reported in deaf people homozygous or compound heterozygous for mutations in *SLC26A4* (5). Absence of goiter and the mild thyroid organification defect in the propositus' father suggests that iodine can cross the apical border of thyroid cells. This can be explained by alternative splicing of the mutated mRNA, maintaining a limited amount of normal transcript. Alternatively, some iodine passage may occur through diffusion, as in the basolateral transport when NIS is absent, or another apical iodine transporter may take on pendrin's function (37). In fact, studies in our T-PS2 thyrocytes showed that intracellular iodide was able to leave the cell, although more slowly and less efficiently than from normal NT thyrocytes.

The lack of apical pendrin immunoreactivity in the two propositi suggests that pathogenesis in our patients was due not only to functional impairment of pendrin but also to defective plasma membrane targeting (38, 39): T-PS2 thyrocytes did not express enough mature pendrin, as indicated by Western blotting and immunofluorescence, although some mature protein was pro-

duced by alternative splicing. T-PS2 cells also showed Golgi immunofluorescence, indicating retention of severely truncated proteins inside Golgi structures, as reported for other pendrin mutants in transfection studies (38, 39). Interestingly, T-FA6 cells overexpress mature pendrin, although it seems to be retained intracellularly, a finding that could be important in the pathophysiology of cold adenomas.

In conclusion, we have described two families with PS from Galicia. The founder mutation c.279delT was detected in both families. A novel mutation, c.416–1G→A, affecting *SLC26A4* splicing, was also found; absence of goiter in subjects homozygous for this mutation could be explained by incomplete penetrance. Some affected subjects have goiter with normal TSH and normal thyroid hormones or hypothyroxinemia. An increase in D1 and D2 expression and activity and in MCT8 expression was found in thyroid tissue of the proposita of family A. These changes are adaptive responses to maintain a normal T_3 supply at the expense of T_4. No pendrin immunoreactivity was seen at the luminal border of follicles in the propositi's thyroid glands, and T-PS2 thyrocytes showed pendrin retention in Golgi structures, indicating that mutations affect targeting of pendrin to the plasma membrane. Pendred-affected thyrocytes showed low iodide efflux and consequent accumulation, confirming the importance of pendrin as an iodide transporter.

Acknowledgments

We thank the members of the two families for their willingness to participate in the study and Xiao-Hui Liao from the Thyroid Study Unit at the University of Chicago for comments.

Address all correspondence and requests for reprints to: Joaquin Lado-Abeal, M.D., Ph.D., Unidade de Enfermedades Tiroideas e Metabólicas, Department of Medicine, University of Santiago de Compostela, C/ San Francisco sn, Santiago de Compostela 15705, Spain. E-mail: melado61@usc.es.

This study was supported by FIS PI030401 (to J.L.-A.) and PI060209 (to J.C.T.), Xunta de Galicia PGIDIT04PXIC20801PN (to J.L.-A.), PGIDIT03PX191801PR (to D.A.-V.), and PGIDIT05BTF20803P (to C.V.A.), Ministerio de Educuación y Ciencia SAF2004-03131 and SAF2006-01319 (to M.J.O.), CMKP 501-2-1-22-05/-12/06 (to B.C.), and National Institutes of Health Grants DK15070 (to S.R.) and RR00055 (to S.R.).

Disclosure Statement: The authors have nothing to disclose.

References

1. **Pendred V** 1896 Deaf mutism and goitre. Lancet 2:532
2. **Everett LA, Glaser B, Beck JC, Idol JR, Buchs A, Heyman M, Adawi F, Hazani E, Nassir E, Baxevanis AD, Sheffield VC, Green ED** 1997 Pendred syndrome is caused by mutations in a putative sulphate transporter gene (PDS). Nat Genet 17:411–422
3. **Everett LA, Belyantseva IA, Noben-Trauth K, Cantos R, Chen A, Thakkar SI, Hoogstraten-Miller SL, Kachar B, Wu DK, Green ED** 2001 Targeted disruption of mouse Pds provides insight about the inner-ear defects encountered in Pendred syndrome. Hum Mol Genet 10:153–161
4. **Friedman TB, Griffith AJ** 2003 Human nonsyndromic sensorineural deafness. Annu Rev Genomics Hum Genet 4:341–402
5. **Albert S, Blons H, Jonard L, Feldmann D, Chauvin P, Loundon N, Sergent-Allaoui A, Houang M, Joannard A, Schmerber S, Delobel B, Leman J, Journel H, Catros H, Dollfus H, Eliot MM, David A, Calais C, Drouin-Garraud V, Obstoy MF, Tran Ba Huy P, Lacombe D, Duriez F, Francannet C, Bitoun P, Petit C, Garabedian EN, Couderc R, Marlin S, Denoyelle F** 2006 SLC26A4 gene is frequently involved in nonsyndromic hearing impairment with enlarged vestibular aqueduct in Caucasian populations. Eur J Hum Genet 14:773–779
6. **Van Hauwe P, Everett LA, Coucke P, Scott DA, Kraft ML, Ris-Stalpers C, Bolder C, Otten B, de Vijlder JJ, Dietrich NL, Ramesh A, Srisailapathy SC, Parving A, Cremers CW, Willems PJ, Smith RJ, Green ED, Van Camp G** 1998 Two frequent missense mutations in Pendred syndrome. Hum Mol Genet 7:1099–1104
7. **Coyle B, Reardon W, Herbrick JA, Tsui LC, Gausden E, Lee J, Coffey R, Grueters A, Grossman A, Phelps PD, Luxon L, Kendall-Taylor P, Scherer SW, Trembath RC** 1998 Molecular analysis of the PDS gene in Pendred syndrome. Hum Mol Genet 7:1105–1112
8. **Kopp P, Karamanoglu Arseven O, Sabacan L, Kotlar T, Dupuis J, Cavaliere H, Santos CLS, Jameson JL, Medeiros-Neto G** 1999 Phenocopies for deafness and goiter development in a large inbred Brazilian kindred with Pendred's syndrome associated with a novel mutation in the PDS gene. J Clin Endocrinol Metab 84:336–341
9. **Usami S, Abe S, Weston MD, Shinkawa H, Van Camp G, Kimberling WJ** 1999 Non-syndromic hearing loss associated with enlarged vestibular aqueduct is caused by PDS mutations. Hum Genet 104:188–192
10. **Fugazzola L, Mannavola D, Cerutti N, Maghnie M, Pagella F, Bianchi P, Weber G, Persani L, Beck-Peccoz P** 2000 Molecular analysis of the Pendred's syndrome gene and magnetic resonance imaging studies of the inner ear are essential for the diagnosis of true Pendred's syndrome. J Clin Endocrinol Metab 85:2469–2475
11. **Adato A, Raskin L, Petit C, Bonne-Tamir B** 2000 Deafness heterogeneity in a Druze isolate from the Middle East: novel OTOF and PDS mutations, low prevalence of GJB2 35delG mutation and indication for a new DFNB locus. Eur J Hum Genet 8:437–442
12. **Gonzalez Trevino O, Karamanoglu Arseven O, Ceballos CJ, Vives VI, Ramirez RC, Gomez VV, Medeiros-Neto G, Kopp P** 2001 Clinical and molecular analysis of three Mexican families with Pendred's syndrome. Eur J Endocrinol 144:585–593
13. **Lopez-Bigas N, Melchionda S, de Cid R, Grifa A, Zelante L, Govea N, Arbonés ML, Gasparini P, Estivill X** 2002 Identification of five new mutations of PDS/SLC26A4 in Mediterranean families with hearing impairment. Hum Mutat 20:77–78
14. **Park H-J, Shaukat S, Liu XZ, Hahn SH, Naz S, Ghosh M, Kim HN, Moon SK, Abe S, Tukamoto K, Riazuddin S, Kabra M, Erdenetungalag R, Radnaabazar J, Khan S, Pandya A, Usami SI, Nance WE, Wilcox ER, Riazuddin S, Griffith AJ** 2003 Origins and frequencies of SLC26A4 (PDS) mutations in east and south Asians: global implications for the epidemiology of deafness. J Med Genet 40:242–248
15. **Borck G, Roth C, Martine U, Wildhardt G, Pohlenz J** 2003 Mutations in the PDS gene in German families with Pendred's syndrome: V138F is a founder mutation. J Clin Endocrinol Metab 88:2916–2921
16. **Blons H, Feldmann D, Duval V, Messaz O, Denoyelle F, Loundon N, Sergout-Allaoui A, Houang M, Duriez F, Lacombe D, Delobel B, Leman J, Catros H, Journel H, Drouin-Garraud V, Obstoy MF, Toutain A, Oden S, Toublanc JE, Couderc R, Petit C, Garabedian EN, Marlin S** 2004 Screening of SLC26A4 (PDS) gene in Pendred's syndrome: a large spectrum of mutations in France and phenotypic heterogeneity. Clin Genet 66:333–340
17. **Prasad S, Kolln KA, Cucci RA, Trembath RC, Van Camp G, Smith RJ** 2004 Pendred syndrome and DFNB4-mutation screening of SLC26A4 by denaturing high-performance liquid chromatography and the identification of eleven novel mutations. Am J Med Genet 124A:1–9
18. **Royaux IE, Suzuki K, Mori A, Katoh R, Everett LA, Kohn LD, Green ED** 2000 Pendrin, the protein encoded by the Pendred syndrome gene (PDS), is an apical porter of iodide in the thyroid and is regulated by thyroglobulin in FRTL-5 cells. Endocrinology 141:839–845
19. **Reardon W, Coffey R, Chowdhury T, Grossman A, Jan H, Britton K, Kendall-Taylor P, Trembath R** 1999 Prevalence, age of onset, and natural history of thyroid disease in Pendred syndrome. J Med Genet 36:595–598
20. **Pisarev MA, Utiger RD, Salvaneschi JP, Altschuler N, DeGroot LJ** 1970 Serum TSH and thyroxine in goitrous subjects in Argentina. J Clin Endocrinol 30: 680–681
21. **Livak KJ, Schmittgen TD** 2001 Analysis of relative gene expression data using real-time quantitative PCR and the $2^{-\Delta\Delta C}$T method. Methods 25:402–408
22. **Weeke J, Orskov H** 1973 Synthesis of monolabeled 3,5,3′-triiodothyronine and thyroxine of maximum specific activity for radioimmunoassay. Scand J Clin Lab Invest 32:357–360
23. **Salvatore D, Tu H, Harney JW, Larsen PR** 1996 Type 2 iodothyronine deiodinase is highly expressed in human thyroid. J Clin Invest 98:962–968
24. **Obregón MJ, Ruiz de Ona C, Calvo R, Escobar del Rey F, Morreale de Escobar**

G 1991 Outer ring iodothyronine deiodinases and thyroid hormone economy: responses to iodine deficiency in the rat fetus and neonate. Endocrinology 129:2663–2673

25. **Skubis-Zegadlo J, Nikodemska A, Przytula E, Mikula M, Bardadin K, Ostrowski J, Wenzel BE, Czarnocka B** 2005 Expression of pendrin in benign and malignant human thyroid tissues. B J Cancer 93:144–151
26. **Bravo SB, Pampin S, Cameselle-Teijeiro J, Carneiro C, Dominguez F, Barreiro F, Alvarez CV** 2003 TGF-β-induced apoptosis in human thyrocytes is mediated by p27kip1 reduction and is overridden in neoplastic thyrocytes by NF-κB activation. Oncogene 22:7819–7830
27. **Bravo SB, Garcia-Rendueles ME, Seoane R, Dosil V, Cameselle-Teijeiro J, Lopez-Lazaro L, Zalvide J, Barreiro F, Pombo CM, Alvarez CV** 2005 Plitidepsin has a cytostatic effect in human undifferentiated (anaplastic) thyroid carcinoma. Clin Cancer Res 11:7664–7673
28. **Garcia A, Alvarez CV, Smith RG, Dieguez C** 2001 Regulation of pit-1 expression by ghrelin and GHRP-6 through the GH secretagogue receptor. Mol Endocrinol 15:1484–1495
29. **Dohan O, De la Vieja A, Carrasco N** 2006 Hydrocortisone and purinergic signaling stimulate sodium/iodide symporter (NIS)-mediated iodide transport in breast cancer cells. Mol Endocrinol 20:1121–1137
30. **Loidi L, Quinteiro C, Parajes S, Barreiro J, Leston DG, Cabezas-Agricola JM, Sueiro AM, Araujo-Vilar D, Catro-Feijoo L, Costas J, Pombo M, Dominguez F** 2006 High variability in CYP21A2 mutated alleles in Spanish 21-hydroxylase deficiency patients, six novel mutations and a founder effect. Clin Endocrinol (Oxf) 64:330–336
31. **Obregon MJ, Escobar del Rey F, Morreale de Escobar G** 2005 The effects of iodine deficiency on thyroid hormone deiodination. Thyroid 5:917–929
32. **Pedraza PE, Obregon MJ, Escobar-Morreale HF, Del Rey FE, de Escobar GM** 2006 Mechanisms of adaptation to iodine deficiency in rats: thyroid status is tissue-specific. Its relevance for man. Endocrinology 147:2098–2108
33. **Li M, Liu DR, Qu CY, Zhang PY, Qian QD, Zhang CD, Jia QZ, Wang HX, Eastman CJ, Boyages SC** 1987 Endemic goitre in central China caused by excessive iodine intake. Lancet 2:257–259
34. **Smerdely P, Pitsiavas V, Boyages SC** 1993 Evidence that the inhibitory effects of iodide on thyroid cell proliferation are due to arrest of the cell cycle at G0G1 and G2M phases. Endocrinology 133:2881–2888
35. **Dugrillon A, Gartner R** 1992 The role of iodine and thyroid cell growth. Thyroidology 4:31–36
36. **Gartner R, Greil W, Demharter R, Horn K** 1985 Involvement of cyclic AMP, iodide and metabolites of arachidonic acid in the regulation of cell proliferation of isolated porcine thyroid follicles. Mol Cell Endocrinol 42:145–155
37. **Rodriguez AM, Perron B, Lacroix L, Caillou B, Leblanc G, Schlumberger M, Bidart JM, Pourcher T** 2002 Identification and characterization of a putative human iodide transporter located at the apical membrane of thyrocytes. J Clin Endocrinol Metab 87:3500–35003
38. **Taylor JP, Metcalfe RA, Watson PF, Weetman AP, Trembath RC** 2002 Mutations of the PDS gene, encoding pendrin, are associated with pendrin mislocalization and loss of iodide efflux: implications for thyroid dysfunction in Pendred syndrome. J Clin Endocrinol Metab 87:1778–1784
39. **Rotman-Pikielny P, Hirschberg K, Maruvada P, Suzuki K, Royaux IE, Green ED, Kohn LD, Lippincott-Schwartz J, Yen PM** 2002 Retention of pendrin in the endoplasmic reticulum is a major mechanism for Pendred syndrome. Hum Mol Genet 11:2625–2633